Interface-penalty finite element methods for interface problems in H^1, $\boldsymbol{H}(\mathbf{curl})$, and $\boldsymbol{H}(\mathrm{div})$ ⋆

Huqing Liu[a,b], Linbo Zhang[a,b], Xiaodi Zhang[a,b], Weiying Zheng[a,b,*]

[a] *LSEC, NCMIS, Institute of Computational Mathematics and Scientific/Engineering Computing, Academy of Mathematics and System Sciences, Chinese Academy of Sciences, Beijing, 100190, China.*
[b] *School of Mathematical Science, University of Chinese Academy of Sciences, Beijing 100049, China.*

Abstract

In this article, interface-penalty finite element methods are proposed to solve interface problems in H^1, $\boldsymbol{H}(\mathbf{curl})$, $\boldsymbol{H}(\mathrm{div})$ spaces on unfitted tetrahedral meshes. The transmission conditions across the interface are derived in a unified framework for three types of interface problems. Usually, the well-posedness of an H^1-elliptic problem requires two transmission conditions for both the solution and the normal flux. The well-posedness for $\boldsymbol{H}(\mathbf{curl})$- or $\boldsymbol{H}(\mathrm{div})$-elliptic problem requires three transmission conditions. This provides the guideline for designing stable high-order finite element methods on unfitted meshes. Optimal error estimates are proven in energy norms for interface-penalty finite element methods within a unified framework for H^1, $\boldsymbol{H}(\mathbf{curl})$, and $\boldsymbol{H}(\mathrm{div})$. All error estimates are independent of the location of the interface relative to the mesh. High-order numerical quadrature rules are employed to compute surface integrals and volume integrals in subdomains with curved boundaries which are produced by the intersection of the interface and the tetrahedral mesh. Numerical examples show optimal convergence of the proposed finite element methods for piecewise smooth solutions.

Keywords: Interface problem, unfitted mesh, interface-penalty finite element method, Maxwell's equation, Nitsche's method

1. Introduction

Interface problems have a variety of applications in science and engineering. For example, each element of a phased-array antenna has curved shape (see Figure 1). The partial differential equations describing these applications usually have discontinuous coefficients across the interfaces. Due to low global regularity of solution and irregular geometry of interface, it is challenging to design highly efficient numerical methods for such equations.

Over the past decades, various numerical approaches have been proposed for solving $H^1(\Omega)$-elliptic interface problems in the literature. In general, these methods can be roughly classified into body-fitted and unfitted methods. For body-fitted method, meshes aligned with the interface are used so as to resolve the discontinuities,

⋆This work was supported by the National Science Fund for Distinguished Young Scholars 11725106, National Key Research and Development Program of China 2016YFB0201304, China NSF grants 91430215, 91530323, 11831016.
*Corresponding author: zwy@lsec.cc.ac.cn (W. Zheng)
Email address: liuhq@lsec.cc.ac.cn (H. Liu), zlb@lsec.cc.ac.cn (L. Zhang), zhangxiaodi@lsec.cc.ac.cn (X. Zhang), zwy@lsec.cc.ac.cn (W. Zheng) (Weiying Zheng)

and the interface conditions or transmission conditions can be easily incorporated into numerical schemes. However, it is usually a nontrivial and time-consuming task to generate body-fitted meshes, especially when complex and moving interfaces are involved. To remedy the challenge of mesh generation, the so-called unfitted methods, in which the interface is allowed to cross mesh elements, have gained much attention. Examples of such methods are the immersed boundary method [14], the immersed interface method [16], the ghost fluid method [17], the immersed finite element method [15], the multiscale finite element method [18], the penalty finite element method [19], the matched interface and boundary method [20], the extended finite element method [21].

Figure 1: Geometric shape of an antenna element

The unfitted interface-penalty finite element method employ an alternative idea to handle interface problems, sometimes also known as CutFEM [24, 25] or Nitsche-XFEM [22, 23]. It is firstly proposed by Hansbo and Hansbo in [4] to solve elliptic interface problems. The idea behind is mainly to double the degrees of freedom (DOFs) on interface elements and then add penalty terms to weakly enforce transmission conditions across the interface. In [4], the authors showed optimal convergence rate without restrictions on the location of the interface. From this perspective, numerous variants for elliptic interface problems have been extensively studied in the past few decades. The robust forms of this method were given in [38, 37]. In these papers, a particular choice of weights for the averaging operator is used which leads to robustness properties both with respect to the discontinuous coefficients and the interface location. Meanwhile, Burman et al introduced an unfitted method with averages and stabilization techniques for arbitrarily high-contrast problems [13]. In [5], an unfitted interior penalty discontinuous Galerkin method is studied for elliptic interface problems and optimal h-convergence for arbitrary p is proven in energy norm and L^2-norm. An unfitted hp interface-penalty finite element method for elliptic interface problems is studied for both two and three dimensions in [7]. Recently, Huang et al used the trick of merging elements to improve the condition number of the stiffness matrix and adopted the technique of harmonic weighting fluxes to deal with the jump of discontinuous coefficients [8]. About the literature on unfitted interface-penalty finite element methods, we also refer to [26, 27] for elasticity problems, to [29, 31, 28, 34] Stokes and Navier-Stokes type problems, to [35, 36] for two-phase and fluid-structure interaction problems, and to [24, 25] for overviews.

In [6], Chen et al proposed an adaptive immersed interface finite element method based on a posteriori error estimates for elliptic and Maxwell equations with discontinuous coefficients and homogeneous transmission conditions. The unfitted mesh is locally refined near the interface to reduce the error based on a posterior error indicators. In [10], Chen et al studied finite element methods for time-dependent Maxwell equations with discontinuous coefficients on both matching and non-matching meshes. In [11, 12], Hiptmair et al proved optimal convergence for $\boldsymbol{H}(\mathbf{curl}, \Omega)$- and $\boldsymbol{H}(\mathrm{div}, \Omega)$-elliptic interface problems with homogeneous jump conditions across the interface using lowest order face or edge elements.

To our best knowledge, it seems that no work on high-order finite element methods exist in the literature for $\boldsymbol{H}(\mathbf{curl}, \Omega)$- and $\boldsymbol{H}(\mathrm{div}, \Omega)$-interface problems. The purpose of this paper is to propose high-order finite element methods for H^1-, $\boldsymbol{H}(\mathbf{curl})$-, and $\boldsymbol{H}(\mathrm{div})$-interface problems on unfitted tetrahedral meshes within a unified framework. Generally, the well-posedness of H^1-elliptic problem needs two transmission conditions across the interface for both the solution and the normal flux. However, the well-posedness of $\boldsymbol{H}(\mathbf{curl})$- or $\boldsymbol{H}(\mathrm{div})$-elliptic problem needs three transmission conditions across the interface. This inspires us to use three types of penalty terms in designing high-order finite element methods for $\boldsymbol{H}(\mathbf{curl})$- and $\boldsymbol{H}(\mathrm{div})$-elliptic problems. Another challenging issue in high-order finite element methods for three-dimensional (3D) interface problems is to develop high-order numerical quadratures on tetrahedra intersected by the interface. Using unfitted meshes, one has to compute integrals accurately both on the curved interface and in the volume of a tetrahedron cut by the interface.

The contributions of the paper are listed as follows:

1. We propose a unified framework for transmission conditions for H^1-, $\boldsymbol{H}(\mathbf{curl})$-, and $\boldsymbol{H}(\mathrm{div})$-interface problems. Different from H^1-interface problem, both $\boldsymbol{H}(\mathbf{curl})$- and $\boldsymbol{H}(\mathrm{div})$-interface problems require three types of transmission conditions across the interface. The well-posedness of interface problems is shown.

2. By introducing interface-penalty terms associated with the transmission conditions, we propose a high-order symmetric interface-penalty finite element method (SIPFEM) and a high-order non-symmetric interface-penalty finite element method (NIPFEM). The well-posedness of discrete problems and the stability of discrete solutions are shown in a unified framework.

3. Optimal error estimates are obtained in energy norms. Moreover, optimal $\boldsymbol{L}^2$-error estimates are obtained for SIPFEM, while sub-optimal $\boldsymbol{L}^2$-error estimates are obtained for NIPFEM with half an order lower than the optimal one. The error estimates are independent of the position of interface relative to meshes.

4. We propose high-order numerical quadrature rules to compute surface integrals and volume integrals in sub-domains with curved boundaries.

Moreover, by numerical experiments for piecewise smooth solutions, we show that optimal convergence rates are obtained for discrete solutions in both $\boldsymbol{L}^2$- and energy norms.

The rest of this paper is organized as follows: In Section 2, we propose H^1-, $\boldsymbol{H}(\mathbf{curl})$-, and $\boldsymbol{H}(\mathrm{div})$-interface problems in a unified framework. The well-posedness of the interface problems is proven. In Section 3, we

propose two interface-penalty finite element methods on unfitted tetrahedral meshes. The well-posedness of discrete problems is shown. In Section 4, we prove the error estimates for both symmetric and non-symmetric schemes. In Section 5, we present high-order numerical quadrature rules for surface integrals and volume integrals in sub-domains with curved boundaries. Numerical examples are provided to show optimal convergence rates of discrete solutions. Finally, we conclude the main result in Section 6. Throughout this paper, we use boldface symbols for vector-valued quantities, such as $\boldsymbol{L}^2(\Omega) = (L^2(\Omega))^3$.

2. The model problems

Let $\Omega \subset \mathbb{R}^3$ be a bounded Lipschitz domain with boundary $\Gamma := \partial\Omega$. Let $\Sigma \subset \Omega$ be a C^2-smooth internal interface which separates Ω into two nonintersecting *open sub-domains* Ω_1 and Ω_2 (see Figure 2 for an illustration). We shall study interface problems proposed on $\Omega_1 \cup \Omega_2$.

For a bounded domain $G \subset \mathbb{R}^3$, let $L^2(G)$ be the Hilbert space of square-integrable functions and denote its inner product by $(u, v)_G$. The notation is abbreviated to $(u, v) := (u, v)_\Omega$ for $G = \Omega$. Define

$$\boldsymbol{H}(\mathrm{d}, G) := \{\boldsymbol{v} \in \boldsymbol{L}^2(G) : \mathrm{d}\boldsymbol{v} \in \boldsymbol{L}^2(\Omega)\}, \qquad \mathrm{d} = \mathbf{grad},\ \mathbf{curl},\ \mathrm{div}\,.$$

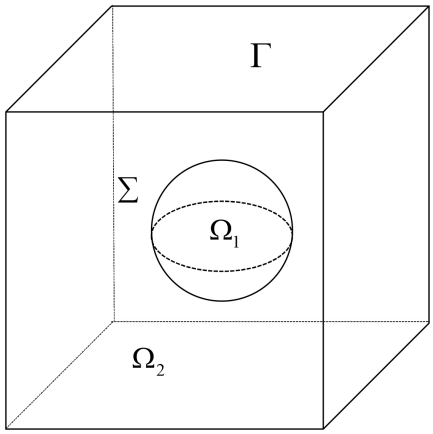

Figure 2: An illustration of the geometry description

2.1. Trace operators

Suppose ∂G is Lipschitz continuous and let Div, Curl be the surface divergence operator and the surface scalar curl operator. From [2], the trace mappings are surjective

$$\begin{aligned}
\gamma :\ & H^1(G) \to H^{1/2}(\partial G), && \gamma\varphi = \varphi \quad \text{on } \partial G,\\
\gamma_{\boldsymbol{n}} :\ & \boldsymbol{H}(\mathrm{div}, G) \to H^{-1/2}(\partial G), && \gamma_{\boldsymbol{n}}\boldsymbol{u} = \boldsymbol{n}\cdot\boldsymbol{u} \quad \text{on } \partial G,\\
\gamma_t :\ & \boldsymbol{H}(\mathbf{curl}, G) \to \boldsymbol{H}^{-1/2}(\mathrm{Div}, \partial G), && \gamma_t\boldsymbol{u} = \boldsymbol{n}\times\boldsymbol{u} \quad \text{on } \partial G,\\
\gamma_T :\ & \boldsymbol{H}(\mathbf{curl}, G) \to \boldsymbol{H}^{-1/2}(\mathrm{Curl}, \partial G), && \gamma_T\boldsymbol{u} = \boldsymbol{n}\times(\boldsymbol{u}\times\boldsymbol{n}) \quad \text{on } \partial G,
\end{aligned}$$

where $\boldsymbol{n}$ is the unit outer normal to G and

$$\boldsymbol{H}^{-1/2}(\mathrm{D},\partial G)=\left\{\boldsymbol{\xi}\in\boldsymbol{H}^{-1/2}(\partial G):\mathrm{D}\boldsymbol{\xi}\in H^{-1/2}(\partial G)\right\}\quad\text{for D}=\mathrm{Div},\ \mathrm{Curl}\,.$$

For $\mathrm{d}\in\{\mathbf{grad},\mathbf{curl},\mathrm{div}\}$, let γ_{d} denote the trace operator on $\boldsymbol{H}(\mathrm{d},G)$, namely,

$$\gamma_{\mathbf{grad}}=\gamma,\quad \gamma_{\mathbf{grad}^*}=\gamma_{-\,\mathrm{div}}=-\gamma_{\mathrm{div}}=-\gamma_{\boldsymbol{n}},\quad \gamma_{\mathbf{curl}}=\gamma_T,\quad \gamma_{\mathbf{curl}^*}=\gamma_t,$$

where d^* is the dual operator of d. For convenience, we shall use the notations

$$\begin{aligned}&\gamma_{\mathbf{grad}}H^1(G)=H^{1/2}(\partial G),&&\gamma_{\mathrm{div}}\boldsymbol{H}(\mathrm{div},G)=H^{-1/2}(\partial G),\\&\gamma_{\mathbf{curl}}\boldsymbol{H}(\mathbf{curl},G)=\boldsymbol{H}^{-1/2}(\mathrm{Curl},\partial G),&&\gamma_{\mathbf{curl}^*}\boldsymbol{H}(\mathbf{curl},G)=\boldsymbol{H}^{-1/2}(\mathrm{Div},\partial G).\end{aligned}$$

Conventionally, the kernels of trace operators are also denoted by

$$\boldsymbol{H}_0(\mathrm{d},G)=\{\boldsymbol{v}\in\boldsymbol{H}(\mathrm{d},G):\gamma_{\mathrm{d}}\boldsymbol{v}=0\ \text{ on }\partial G\}\,.$$

Since $\boldsymbol{v}=(\gamma_{\boldsymbol{n}}\boldsymbol{v})\boldsymbol{n}+\gamma_T\boldsymbol{v}$ on ∂G, $\boldsymbol{H}_0(\mathbf{curl},G)$ can also be identified with

$$\boldsymbol{H}_0(\mathbf{curl},G)=\{v\in\boldsymbol{H}(\mathbf{curl},G):\ \gamma_T\boldsymbol{v}=0\ \text{ on }\partial G\}\,.$$

2.2. Interface problems

For $\mathrm{d}\in\{\mathbf{grad},\mathbf{curl},\mathrm{div}\}$, the $\boldsymbol{H}(\mathrm{d})$-interface problem is proposed on $\Omega_1\cup\Omega_2$ as follows

$$\mathrm{d}^*\left(\alpha\mathrm{d}\boldsymbol{u}\right)+\beta\boldsymbol{u}=\boldsymbol{f}_{\mathrm{d}}\quad\text{in }\Omega_1\cup\Omega_2,\tag{1a}$$

$$[\![\gamma_{\mathrm{d}^*}(\alpha\mathrm{d}\boldsymbol{u})]\!]=\boldsymbol{\psi}_{\mathrm{d}}\quad\text{on }\Sigma,\tag{1b}$$

$$[\![\gamma_{\mathrm{d}}\boldsymbol{u}]\!]=\boldsymbol{\phi}_{\mathrm{d}}\quad\text{on }\Sigma,\tag{1c}$$

$$[\![\gamma_{\mathrm{d}^*_\succ}(\beta\boldsymbol{u}-\boldsymbol{f}_{\mathrm{d}})]\!]=0\quad\text{on }\Sigma,\tag{1d}$$

$$\gamma_{\mathrm{d}}\boldsymbol{u}=0\quad\text{on }\Gamma,\tag{1e}$$

where $\mathrm{d}^*_\succ$ is the succedent operator of d^* in the sequence $\{\mathbf{grad},\mathbf{curl},\mathrm{div}\}$, i.e.

$$\mathbf{grad}_\succ=\mathbf{curl},\qquad\mathbf{curl}_\succ=\mathrm{div},\qquad\mathrm{div}_\succ=0.$$

Here $[\![\boldsymbol{w}]\!]:=\boldsymbol{w}|_{\Omega_1}-\boldsymbol{w}|_{\Omega_2}$ denotes the jump of function $\boldsymbol{w}$ across Σ. The coefficients α and β satisfy, for some constants α_j and β_j,

$$\alpha,\beta\in L^\infty(\Omega),\qquad\alpha\geq\alpha_j>0,\quad\beta\geq\beta_j>0\quad\text{in }\ \Omega_j,\qquad j=1,2.$$

Moreover, we assume that, for $\mathrm{d}\in\{\mathbf{grad},\mathbf{curl},\mathrm{div}\}$,

$$\boldsymbol{f}_{\mathrm{d}}\in\boldsymbol{L}^2(\Omega),\qquad\boldsymbol{\phi}_{\mathrm{d}}\in\gamma_{\mathrm{d},\Sigma}\boldsymbol{H}(\mathrm{d},\Omega_1),\qquad\boldsymbol{\psi}_{\mathrm{d}}\in\gamma_{\mathrm{d}^*,\Sigma}\boldsymbol{H}(\mathrm{d}^*,\Omega_1),$$

where $\gamma_{\mathrm{d},\Sigma}\boldsymbol{H}(\mathrm{d},\Omega_1):=\{\boldsymbol{\xi}|_\Sigma:\boldsymbol{\xi}\in\gamma_{\mathrm{d}}\boldsymbol{H}(\mathrm{d},\Omega_1)\}$.

Now we rewrite (1) into the specific forms for d = **grad**, **curl**, and div. For d = **grad**, (1) stands for second-order elliptic problem. Since $\mathrm{d}^*_{\succ} = -\operatorname{div}_{\succ} = 0$, the jump condition (1d) is not needed any more. So (1) turns out to be

$$
\begin{aligned}
-\operatorname{div}(\alpha\nabla u) + \beta u &= f_{\mathbf{grad}} \quad \text{in } \Omega_1 \cup \Omega_2, && \text{(2a)}\\
-[\![\gamma_{\boldsymbol{n}}(\alpha\nabla u)]\!] &= \psi_{\mathbf{grad}} \quad \text{on } \Sigma, && \text{(2b)}\\
[\![\gamma u]\!] &= \phi_{\mathbf{grad}} \quad \text{on } \Sigma, && \text{(2c)}\\
\gamma u &= 0 \quad \text{on } \Gamma. && \text{(2d)}
\end{aligned}
$$

For d = **curl**, (1) turns into

$$
\begin{aligned}
\mathbf{curl}\,(\alpha\,\mathbf{curl}\,\boldsymbol{u}) + \beta\boldsymbol{u} &= \boldsymbol{f}_{\mathbf{curl}} \quad \text{in } \Omega_1 \cup \Omega_2, && \text{(3a)}\\
[\![\gamma_t(\alpha\,\mathbf{curl}\,\boldsymbol{u})]\!] &= \boldsymbol{\psi}_{\mathbf{curl}} \quad \text{on } \Sigma, && \text{(3b)}\\
[\![\gamma_T\boldsymbol{u}]\!] &= \boldsymbol{\phi}_{\mathbf{curl}} \quad \text{on } \Sigma, && \text{(3c)}\\
[\![\gamma_{\boldsymbol{n}}(\beta\boldsymbol{u} - \boldsymbol{f}_{\mathbf{curl}})]\!] &= 0 \quad \text{on } \Sigma, && \text{(3d)}\\
\gamma_T\boldsymbol{u} &= 0 \quad \text{on } \Gamma. && \text{(3e)}
\end{aligned}
$$

For d = div, (1) turns into

$$
\begin{aligned}
-\nabla(\alpha\operatorname{div}\boldsymbol{u}) + \beta\boldsymbol{u} &= \boldsymbol{f}_{\mathrm{div}} \quad \text{in } \Omega_1 \cup \Omega_2, && \text{(4a)}\\
-[\![\gamma(\alpha\operatorname{div}\boldsymbol{u})]\!] &= \psi_{\mathrm{div}} \quad \text{on } \Sigma, && \text{(4b)}\\
[\![\gamma_{\boldsymbol{n}}\boldsymbol{u}]\!] &= \phi_{\mathrm{div}} \quad \text{on } \Sigma, && \text{(4c)}\\
[\![\gamma_T(\beta\boldsymbol{u} - \boldsymbol{f}_{\mathrm{div}})]\!] &= 0 \quad \text{on } \Sigma, && \text{(4d)}\\
\gamma_{\boldsymbol{n}}\boldsymbol{u} &= 0 \quad \text{on } \Gamma. && \text{(4e)}
\end{aligned}
$$

2.3. Weak formulation

To derive a weak formulation for (1), or for (2)–(4), we shall use the space of piecewise regular functions

$$
\begin{aligned}
\boldsymbol{H}(\mathrm{d},\Omega_1,\Omega_2) &= \left\{\boldsymbol{v}\in\boldsymbol{L}^2(\Omega) : \boldsymbol{v}|_{\Omega_j}\in\boldsymbol{H}(\mathrm{d},\Omega_j),\ j=1,2\right\},\\
\boldsymbol{H}_0(\mathrm{d},\Omega_1,\Omega_2) &= \{\boldsymbol{v}\in\boldsymbol{H}(\mathrm{d},\Omega_1,\Omega_2) : \gamma_{\mathrm{d}}\boldsymbol{v} = 0 \ \text{ on } \Gamma\cap\partial\Omega_j,\ j=1,2\}.
\end{aligned}
$$

The norm on $\boldsymbol{H}(\mathrm{d},\Omega_1,\Omega_2)$ is defined by

$$
\|\boldsymbol{v}\|_{\boldsymbol{H}(\mathrm{d},\Omega_1,\Omega_2)} := \left(\|\boldsymbol{v}\|^2_{\boldsymbol{H}(\mathrm{d},\Omega_1)} + \|\boldsymbol{v}\|^2_{\boldsymbol{H}(\mathrm{d},\Omega_2)}\right)^{1/2}.
$$

Multiplying both sides of (1a) with $\boldsymbol{v}\in\boldsymbol{H}_0(\mathrm{d},\Omega_1,\Omega_2)$ and using integration by part, we find that

$$
\sum_{j=1}^{2}(\alpha\mathrm{d}\boldsymbol{u},\mathrm{d}\boldsymbol{v})_{\Omega_j} + \int_\Sigma [\![\gamma_{\mathrm{d}^*}(\alpha\mathrm{d}\boldsymbol{u})\cdot\gamma_{\mathrm{d}}\boldsymbol{v}]\!] + (\beta\boldsymbol{u},\boldsymbol{v}) = (\boldsymbol{f}_{\mathrm{d}},\boldsymbol{v}).
$$

Let $\{\!\{\xi\}\!\} := (\xi|_{\Omega_1} + \xi|_{\Omega_2})/2$ denote the average of ξ on Σ. Note that

$$
\begin{aligned}
[\![\gamma_{\mathrm{d}^*}(\alpha\mathrm{d}\boldsymbol{u})\cdot\gamma_{\mathrm{d}}\boldsymbol{v}]\!] &= \{\!\{\gamma_{\mathrm{d}^*}(\alpha\mathrm{d}\boldsymbol{u})\}\!\}\cdot[\![\gamma_{\mathrm{d}}\boldsymbol{v}]\!] + [\![\gamma_{\mathrm{d}^*}(\alpha\mathrm{d}\boldsymbol{u})]\!]\cdot\{\!\{\gamma_{\mathrm{d}}\boldsymbol{v}\}\!\}\\
&= \{\!\{\gamma_{\mathrm{d}^*}(\alpha\mathrm{d}\boldsymbol{u})\}\!\}\cdot[\![\gamma_{\mathrm{d}}\boldsymbol{v}]\!] + \boldsymbol{\psi}_{\mathrm{d}}\cdot\{\!\{\gamma_{\mathrm{d}}\boldsymbol{v}\}\!\}.
\end{aligned}
$$

We obtain a weak formulation of (1): Find $\boldsymbol{u} \in \boldsymbol{H}_0(\mathrm{d}, \Omega_1, \Omega_2)$ such that $[\![\gamma_{\mathrm{d}} \boldsymbol{u}]\!] = \boldsymbol{\phi}_{\mathrm{d}}$ on Σ and

$$\mathscr{A}_{\mathrm{d}}(\boldsymbol{u}, \boldsymbol{v}) = \mathcal{L}_{\mathrm{d}}(\boldsymbol{v}) \qquad \forall\, \boldsymbol{v} \in \boldsymbol{H}_0(\mathrm{d}, \Omega_1, \Omega_2), \tag{5}$$

where the bilinear form $\mathscr{A}_{\mathrm{d}}$: $\boldsymbol{H}_0(\mathrm{d}, \Omega_1, \Omega_2) \times \boldsymbol{H}_0(\mathrm{d}, \Omega_1, \Omega_2) \to \mathbb{R}$ and the linear form $\mathcal{L}_{\mathrm{d}} \in [\boldsymbol{H}_0(\mathrm{d}, \Omega_1, \Omega_2)]'$ are defined by

$$\mathscr{A}_{\mathrm{d}}(\boldsymbol{u}, \boldsymbol{v}) := \sum_{j=1}^{2} (\alpha \mathrm{d}\boldsymbol{u}, \mathrm{d}\boldsymbol{v})_{\Omega_j} + (\beta \boldsymbol{u}, \boldsymbol{v}) + \int_{\Sigma} \{\!\{\gamma_{\mathrm{d}^*}(\alpha \mathrm{d}\boldsymbol{u})\}\!\} \cdot [\![\gamma_{\mathrm{d}} \boldsymbol{v}]\!]\,, \tag{6}$$

$$\mathcal{L}_{\mathrm{d}}(\boldsymbol{v}) := (\boldsymbol{f}_{\mathrm{d}}, \boldsymbol{v}) - \int_{\Sigma} \boldsymbol{\psi}_{\mathrm{d}} \cdot \{\!\{\gamma_{\mathrm{d}} \boldsymbol{v}\}\!\}\,. \tag{7}$$

Here $\int_{\Sigma} \boldsymbol{\xi} \cdot \boldsymbol{\eta}$ denotes the duality pairing between $\boldsymbol{\xi}$ and $\boldsymbol{\eta}$. When $\boldsymbol{\xi}, \boldsymbol{\eta} \in L^2(\Sigma)$, the notation is also used to denote the $L^2(\Sigma)$–inner product.

Theorem 2.1. *Problem* (5) *has a unique solution. Moreover, there exists a constant* $C > 0$ *depending only on* Ω_1, Ω_2 *such that*

$$\|\boldsymbol{u}\|_{\boldsymbol{H}(\mathrm{d},\Omega_1,\Omega_2)} \le C \|\boldsymbol{\phi}_{\mathrm{d}}\|_{\gamma_{\mathrm{d}},\Sigma \boldsymbol{H}(\mathrm{d},\Omega_1)} + C \|\boldsymbol{\psi}_{\mathrm{d}}\|_{\gamma_{\mathrm{d}^*},\Sigma \boldsymbol{H}(\mathrm{d}^*,\Omega_1)} + C \|\boldsymbol{f}\|_{\boldsymbol{L}^2(\Omega)}\,.$$

Proof. Let $\boldsymbol{\phi}_1$ be the zero extension of $\boldsymbol{\phi}_{\mathrm{d}}$ to $\partial\Omega_1 \backslash \Sigma$. Since $\gamma_{\mathrm{d}} \boldsymbol{u} = 0$ on $\Gamma \backslash \Sigma$, we have $\boldsymbol{\phi}_1 \in \gamma_{\mathrm{d}} \boldsymbol{H}(\mathrm{d}, \Omega_1)$. There is a lifting $\boldsymbol{w}_1 \in \boldsymbol{H}(\mathrm{d}, \Omega_1)$ such that

$$\gamma_{\mathrm{d}} \boldsymbol{w}_1 = \boldsymbol{\phi}_1 \quad \text{on } \partial\Omega_1, \qquad \|\boldsymbol{w}_1\|_{\boldsymbol{H}(\mathrm{d},\Omega_1)} \le C \|\phi_1\|_{\gamma_{\mathrm{d}} \boldsymbol{H}(\mathrm{d},\Omega_1)}\,.$$

Let $\boldsymbol{w}$ be the zero extension of $\boldsymbol{w}_1$ to Ω_2. Then we have $\boldsymbol{w} \in \boldsymbol{H}_0(\mathrm{d}, \Omega_1, \Omega_2)$ and $[\![\boldsymbol{w}]\!] = [\![\boldsymbol{u}]\!]$ on Σ. So $\hat{\boldsymbol{u}} := \boldsymbol{u} - \boldsymbol{w} \in \boldsymbol{H}_0(\mathrm{d}, \Omega)$.

We can write (5) into an equivalent form: Find $\hat{\boldsymbol{u}} \in \boldsymbol{H}_0(\mathrm{d}, \Omega)$ such that

$$(\alpha \mathrm{d}\hat{\boldsymbol{u}}, \mathrm{d}\boldsymbol{v}) + (\beta \hat{\boldsymbol{u}}, \boldsymbol{v}) = \mathcal{L}_{\mathrm{d}}(\boldsymbol{v}) - \sum_{j=1}^{2} (\alpha \mathrm{d}\boldsymbol{w}, \mathrm{d}\boldsymbol{v})_{\Omega_j} - (\beta \boldsymbol{w}, \boldsymbol{v}) \quad \forall\, \boldsymbol{v} \in \boldsymbol{H}_0(\mathrm{d}, \Omega). \tag{8}$$

The left-hand side provides a continuous and coercive bilinear form and the right-hand side provides a continuous linear functional on $\boldsymbol{H}_0(\mathrm{d}, \Omega)$. So (8) has a unique solution. Therefore, (5) has a unique solution. The proof for the stability is easy. □

3. Finite element approximations

In this section, we propose two unfitted interface-penalty finite element methods for solving (1).

Let $\{\mathcal{T}_h\}$ be a family of conforming, quasi-uniform, and shape-regular partition of Ω into closed tetrahedra. Let $h_K = \mathrm{diam}\,(K)$ denote the diameter of $K \in \mathcal{T}_h$ and $h := \max_{K \in \mathcal{T}_h} h_K$ the maximal diameter. The set of all tetrahedra that intersect the interface is denoted by

$$\mathcal{T}_{h,\Sigma} := \{K \in \mathcal{T}_h : \mathrm{area}(K \cap \Sigma) > 0\}\,.$$

Clearly $\mathcal{T}_{h,\Sigma}$ generates a partition of Σ which is denoted by

$$\mathcal{S}_h := \{\mathrm{f} :\ \mathrm{f} = K \cap \Sigma,\ \forall K \in \mathcal{T}_{h,\Sigma}\}\,.$$

It is reasonable to assume that each $\mathrm{f} \in \mathcal{S}_h$ satisfies one of the two cases:

- the interior of f is entirely included in the interior of an element $K^{\mathrm{f}} \in \mathcal{T}_h$, or
- $\mathrm{f} = \partial K_1^{\mathrm{f}} \cap \partial K_2^{\mathrm{f}}$ for two tetrahedra $K_1^{\mathrm{f}}, K_2^{\mathrm{f}} \in \mathcal{T}_h$.

We also write $K_j^{\mathrm{f}} := K^{\mathrm{f}} \cap \Omega_j$, $j = 1, 2$ in the first case. So for both cases, we have

$$\mathrm{f} = \partial K_1^{\mathrm{f}} \cap \partial K_2^{\mathrm{f}}, \quad K_j^{\mathrm{f}} \subset \bar{\Omega}_j, \quad j = 1, 2. \tag{9}$$

Naturally, $\mathcal{T}_h$ generates the partitions of Ω_1 and Ω_2

$$\mathcal{T}_j = \{K \cap \Omega_j : \forall\, K \in \mathcal{T}_h\}, \qquad j = 1, 2.$$

For simplicity, we also assume that α and β are piecewise constants in the neighborhood of Σ, more precisely, there are constants $\alpha_j > 0$, $\beta_j > 0$ such that

$$\alpha \equiv \alpha_j, \quad \beta \equiv \beta_j \quad \text{in } K \cap \Omega_j, \quad \forall\, K \in \mathcal{T}_{h,\Sigma}, \ \ j = 1, 2. \tag{10}$$

3.1. Interface-penalty finite element methods

For any integer $k \geq 0$, let P_k denote the space of polynomials of degrees no more than k and define $\boldsymbol{P}_k = (P_k)^3$. The unfitted finite element space for the discretization of (5) is defined by

$$\boldsymbol{U}^h(k; \mathrm{d}) := \{\boldsymbol{v} \in \boldsymbol{H}_0(\mathrm{d}, \Omega_1, \Omega_2) : \boldsymbol{v}|_K \in \boldsymbol{P}_k(K),\ \forall\, K \in \mathcal{T}_1 \cup \mathcal{T}_2\}\,.$$

The interface-penalty finite element approximation to problem (5) reads: Find $\boldsymbol{u}_h \in \boldsymbol{U}^h(k; \mathrm{d})$ such that

$$\mathscr{A}_{\mathrm{d}}^h(\boldsymbol{u}_h, \boldsymbol{v}_h) = \mathcal{L}_{\mathrm{d}}^h(\boldsymbol{v}_h) \qquad \forall\, \boldsymbol{v}_h \in \boldsymbol{U}^h(k; \mathrm{d}), \tag{11}$$

where the discrete bilinear form $\mathscr{A}_{\mathrm{d}}^h$ is defined by

$$\begin{aligned}
\mathscr{A}_{\mathrm{d}}^h(\boldsymbol{u}_h, \boldsymbol{v}_h) :=& \sum_{j=1}^{2} (\alpha \mathrm{d}\boldsymbol{u}_h, \mathrm{d}\boldsymbol{v}_h)_{\Omega_j} + (\beta \boldsymbol{u}_h, \boldsymbol{v}_h) + \sum_{j=0}^{2} \mathscr{J}_j(\boldsymbol{u}_h, \boldsymbol{v}_h) \\
&+ \sum_{\mathrm{f} \in \mathcal{S}_h} \int_{\mathrm{f}} \left(\{\!\{ \gamma_{\mathrm{d}^*}(\alpha \mathrm{d}\boldsymbol{u}_h) \}\!\} \cdot [\![\gamma_{\mathrm{d}} \boldsymbol{v}_h]\!] + s\, \{\!\{ \gamma_{\mathrm{d}^*}(\alpha \mathrm{d}\boldsymbol{v}_h) \}\!\} \cdot [\![\gamma_{\mathrm{d}} \boldsymbol{u}_h]\!] \right), \\
\mathscr{J}_0(\boldsymbol{u}_h, \boldsymbol{v}_h) :=& \lambda \sum_{\mathrm{f} \in \mathcal{S}_h} \frac{k^2}{h} \int_{\mathrm{f}} [\![\gamma_{\mathrm{d}} \boldsymbol{u}_h]\!] \cdot [\![\gamma_{\mathrm{d}} \boldsymbol{v}_h]\!]\,, \\
\mathscr{J}_1(\boldsymbol{u}_h, \boldsymbol{v}_h) :=& \sum_{\mathrm{f} \in \mathcal{S}_h} \frac{h}{k^2} \int_{\mathrm{f}} [\![\gamma_{\mathrm{d}^*}(\alpha \mathrm{d}\boldsymbol{u}_h)]\!] \cdot [\![\gamma_{\mathrm{d}^*}(\alpha \mathrm{d}\boldsymbol{v}_h)]\!]\,, \\
\mathscr{J}_2(\boldsymbol{u}_h, \boldsymbol{v}_h) :=& \sum_{\mathrm{f} \in \mathcal{S}_h} \frac{1}{k^2 h} \int_{\mathrm{f}} \left[\!\!\left[\gamma_{\mathrm{d}_\succ^*}(\beta \boldsymbol{u}_h) \right]\!\!\right] \cdot \left[\!\!\left[\gamma_{\mathrm{d}_\succ^*}(\beta \boldsymbol{v}_h) \right]\!\!\right]\,,
\end{aligned}$$

and the discrete linear form $\mathcal{L}_{\mathrm{d}}^h$ is defined by

$$\begin{aligned}
\mathcal{L}_{\mathrm{d}}^h(\boldsymbol{v}_h) :=& \int_\Omega \boldsymbol{f}_{\mathrm{d}} \cdot \boldsymbol{v}_h + \sum_{j=0}^{2} \mathcal{J}_j(\boldsymbol{v}_h) + \sum_{\mathrm{f} \in \mathcal{S}_h} \int_{\mathrm{f}} \left(s \boldsymbol{\phi}_{\mathrm{d}} \cdot \{\!\{ \gamma_{\mathrm{d}^*}(\alpha \mathrm{d}\boldsymbol{v}_h) \}\!\} - \boldsymbol{\psi}_{\mathrm{d}} \cdot \{\!\{ \gamma_{\mathrm{d}} \boldsymbol{v}_h \}\!\} \right), \\
\mathcal{J}_0(\boldsymbol{v}_h) :=& \lambda \sum_{\mathrm{f} \in \mathcal{S}_h} \frac{k^2}{h} \int_{\mathrm{f}} \boldsymbol{\phi}_{\mathrm{d}} \cdot [\![\gamma_T \boldsymbol{v}_h]\!]\,, \\
\mathcal{J}_1(\boldsymbol{v}_h) :=& \sum_{\mathrm{f} \in \mathcal{S}_h} \frac{h}{k^2} \int_{\mathrm{f}} \boldsymbol{\psi}_{\mathrm{d}} \cdot [\![\gamma_{\mathrm{d}^*}(\alpha \mathrm{d}\boldsymbol{v}_h)]\!]\,, \\
\mathcal{J}_2(\boldsymbol{v}_h) :=& \sum_{\mathrm{f} \in \mathcal{S}_h} \frac{1}{k^2 h} \int_{\mathrm{f}} \left[\!\!\left[\gamma_{\mathrm{d}_\succ^*}(\boldsymbol{f}_{\mathrm{d}}) \right]\!\!\right] \left[\!\!\left[\gamma_{\mathrm{d}_\succ^*}(\beta \boldsymbol{v}_h) \right]\!\!\right]\,.
\end{aligned}$$

Here we assume $\gamma_{\mathrm{d}^*_\succ}(\boldsymbol{f}_{\mathrm{d}}) \in \left[\boldsymbol{C}^1(\mathrm{f})\right]'$ for any $\mathrm{f} \in \mathcal{S}_h$. This justifies the discrete functional $\mathcal{J}_2$ on $\boldsymbol{U}^h(k;\mathrm{d})$.

For $s = 1$, $\mathscr{A}_{\mathrm{d}}^h$ is symmetric and the method is thus called *symmetric interface-penalty finite element method* (SIPFEM). For $s = -1$, the method is called *non-symmetric interface-penalty finite element method* (NIPFEM). In this paper, we only consider the two cases $s = \pm 1$. The theories can be extended to $s \neq \pm 1$ straightforwardly. Here $\mathscr{J}_j$, $j = 0, 1, 2$, are penalty terms added to control the interface jumps in (1b)-(1d) and insure the coercivity of $\mathscr{A}_{\mathrm{d}}^h$, and $\mathcal{J}_j$ are consistent terms associated with $\mathscr{J}_j$. The stabilization parameter $\lambda > 0$ is assumed to be large enough but independent of h.

Using (3b)-(3d) and (5), it is easy to see that the exact solution $\boldsymbol{u}$ satisfies

$$\mathscr{A}_{\mathrm{d}}^h(\boldsymbol{u}, \boldsymbol{v}_h) = \mathcal{L}_{\mathrm{d}}^h(\boldsymbol{v}_h) \qquad \forall \boldsymbol{v}_h \in \boldsymbol{U}^h(k;\mathrm{d}). \tag{12}$$

This yields the Galerkin orthogonality

$$\mathscr{A}_{\mathrm{d}}^h(\boldsymbol{u} - \boldsymbol{u}_h, \boldsymbol{v}_h) = 0 \qquad \forall \boldsymbol{v}_h \in \boldsymbol{U}^h(k;\mathrm{d}). \tag{13}$$

3.2. The well-posedness of (11)

Now we prove the existence, uniqueness, and stability of the discrete solution $\boldsymbol{u}_h$. By the Lax-Milgram lemma, it suffices to prove the coercivity and continuity of $\mathscr{A}_{\mathrm{d}}^h$ and the continuity of $\mathcal{L}_{\mathrm{d}}^h$ under the discrete norm $|||\cdot|||_{1,h}$ which is defined by

$$\begin{aligned}
|||\boldsymbol{v}|||_{1,h}^2 &:= \|\boldsymbol{v}\|_{1,h}^2 + \sum_{\mathrm{f}\in\mathcal{S}_h} \frac{h}{\lambda k^2} \left\|\{\!\{\gamma_{\mathrm{d}^*}(\alpha \mathrm{d}\boldsymbol{v})\}\!\}\right\|_{\boldsymbol{L}^2(\mathrm{f})}^2, \\
\|\boldsymbol{v}\|_{1,h}^2 &:= \sum_{j=1}^{2} \left\|\alpha^{1/2}\mathrm{d}\boldsymbol{v}\right\|_{\boldsymbol{L}^2(\Omega_j)}^2 + \left\|\beta^{1/2}\boldsymbol{v}\right\|_{\boldsymbol{L}^2(\Omega)}^2 + \sum_{j=0}^{2} \mathscr{J}_j(\boldsymbol{v}, \boldsymbol{v}).
\end{aligned}$$

First we cite [8] for the trace inequalities on $\mathcal{I}_h$. They play an important role in proving error estimates for discrete solutions.

Lemma 3.1. *Suppose Σ is C^2-smooth. There exists an $h_0 > 0$ depending only on Σ and the shape regularity of meshes such that, for any $h \in (0, h_0]$ and any $\mathrm{f} \in \mathcal{S}_h$,*

$$\|v\|_{L^2(\mathrm{f})} \leq C_1 h^{-1/2} \|v\|_{L^2(K_j^{\mathrm{f}})} \quad \forall v \in P_k\left(K_j^{\mathrm{f}}\right), \tag{14}$$

$$\|v\|_{L^2(\mathrm{f})} \leq C_2 \left(h^{-1/2} \|v\|_{L^2(K_j^{\mathrm{f}})} + \|v\|_{L^2(K_j^{\mathrm{f}})}^{1/2} \|\nabla v\|_{\boldsymbol{L}^2(K_j^{\mathrm{f}})}^{1/2}\right) \quad \forall v \in H^1(K_1^{\mathrm{f}}, K_2^{\mathrm{f}}), \tag{15}$$

for either $j = 1$ or 2, where K_1^{f}, K_2^{f} are defined in (9)*. The constants C_1, C_2 are independent of h and the location of the interface relative to the mesh.*

Lemma 3.2. *Suppose the penalty parameter $\lambda \geq 2 + 8C_1^2 k^{-2}$. Then $\mathscr{A}_{\mathrm{d}}^h$ satisfies, for any $\boldsymbol{u}, \boldsymbol{v} \in \boldsymbol{U}^h(k;\mathrm{d})$,*

$$\mathscr{A}_{\mathrm{d}}^h(\boldsymbol{v}_h, \boldsymbol{v}_h) \geq \frac{1}{4} |||\boldsymbol{v}_h|||_{1,h}^2, \qquad \left|\mathscr{A}_{\mathrm{d}}^h(\boldsymbol{u}_h, \boldsymbol{v}_h)\right| \leq 2 |||\boldsymbol{u}_h|||_{1,h} |||\boldsymbol{v}_h|||_{1,h}. \tag{16}$$

Proof. We prove the coercivity first. The definition of $\mathscr{A}_{\mathrm{d}}^h$ shows that

$$\begin{aligned}\mathscr{A}_{\mathrm{d}}^h(\boldsymbol{v}_h,\boldsymbol{v}_h) &= \|\boldsymbol{v}_h\|_{1,h}^2 + (1+s)\sum_{\mathrm{f}\in\mathcal{S}_h}\int_{\mathrm{f}}\{\!\{\gamma_{\mathrm{d}^*}(\alpha\mathrm{d}\boldsymbol{v}_h)\}\!\}\cdot[\![\gamma_{\mathrm{d}}\boldsymbol{v}_h]\!]\\ &= |\!|\!|\boldsymbol{v}_h|\!|\!|_{1,h}^2 - \sum_{\mathrm{f}\in\mathcal{S}_h}\frac{h}{\lambda k^2}\|\{\!\{\gamma_{\mathrm{d}^*}(\alpha\mathrm{d}\boldsymbol{v})\}\!\}\|_{\boldsymbol{L}^2(\mathrm{f})}^2\\ &\quad + (1+s)\sum_{\mathrm{f}\in\mathcal{S}_h}\int_{\mathrm{f}}\{\!\{\gamma_{\mathrm{d}^*}(\alpha\mathrm{d}\boldsymbol{v}_h)\}\!\}\cdot[\![\gamma_{\mathrm{d}}\boldsymbol{v}_h]\!]\,. \end{aligned}\tag{17}$$

For any $\mathrm{f}\in\mathcal{S}_h$, assume Lemma 3.1 holds for $j=1$ without loss of generality. Then

$$\{\!\{\gamma_{\mathrm{d}^*}(\alpha\mathrm{d}\boldsymbol{v}_h)\}\!\} = \gamma_{\mathrm{d}^*}\big((\alpha\mathrm{d}\boldsymbol{v}_h)|_{K_1^{\mathrm{f}}}\big) - \frac{1}{2}[\![\gamma_{\mathrm{d}^*}(\alpha\mathrm{d}\boldsymbol{v}_h)]\!] \quad \text{on f.}$$

Since α is constant in K_1^{f} by (10), an application of (14) yields

$$\left\|\gamma_{\mathrm{d}^*}\big((\alpha\mathrm{d}\boldsymbol{v}_h)|_{K_1^{\mathrm{f}}}\big)\right\|_{\boldsymbol{L}^2(\mathrm{f})} \le \left\|(\alpha\mathrm{d}\boldsymbol{v}_h)|_{K_1^{\mathrm{f}}}\right\|_{\boldsymbol{L}^2(\mathrm{f})} \le C_1 h^{-1/2}\left\|\alpha^{1/2}\mathrm{d}\boldsymbol{v}_h\right\|_{\boldsymbol{L}^2(K_1^{\mathrm{f}})}.\tag{18}$$

By the Cauchy-Schwarz inequality, we deduce that

$$\|\{\!\{\gamma_{\mathrm{d}^*}(\alpha\mathrm{d}\boldsymbol{v}_h)\}\!\}\|_{\boldsymbol{L}^2(\mathrm{f})}^2 \;\le\; 2C_1^2h^{-1}\left\|\alpha^{1/2}\mathrm{d}\boldsymbol{v}_h\right\|_{\boldsymbol{L}^2(K_1^{\mathrm{f}})}^2 + 1/2\,\|[\![\gamma_{\mathrm{d}^*}(\alpha\mathrm{d}\boldsymbol{v}_h)]\!]\|_{\boldsymbol{L}^2(\mathrm{f})}^2.$$

Summing the contributions from $\mathrm{f}\in\mathcal{S}_h$ and using $\lambda\ge 2+8C_1^2k^{-2}$, we have

$$\sum_{\mathrm{f}\in\mathcal{S}_h}\frac{h}{\lambda k^2}\|\{\!\{\gamma_{\mathrm{d}^*}(\alpha\mathrm{d}\boldsymbol{v})\}\!\}\|_{\boldsymbol{L}^2(\mathrm{f})}^2 \le \max\left(\frac{2C_1^2}{\lambda k^2},\frac{1}{2\lambda}\right)\|\boldsymbol{v}_h\|_{1,h}^2 \le \frac{1}{4}|\!|\!|\boldsymbol{v}_h|\!|\!|_{1,h}^2.\tag{19}$$

Using (18) and arguments similar to (19), we obtain

$$\begin{aligned}\left|\int_{\mathrm{f}}\{\!\{\gamma_{\mathrm{d}^*}(\alpha\mathrm{d}\boldsymbol{v}_h)\}\!\}\cdot[\![\gamma_{\mathrm{d}}\boldsymbol{v}_h]\!]\right| &\le \|\{\!\{\gamma_{\mathrm{d}^*}(\alpha\mathrm{d}\boldsymbol{v}_h)\}\!\}\|_{\boldsymbol{L}^2(\mathrm{f})}\,\|[\![\gamma_{\mathrm{d}}\boldsymbol{v}_h]\!]\|_{\boldsymbol{L}^2(\mathrm{f})}\\ &\le \frac{1}{8}\left\|\alpha^{1/2}\mathrm{d}\boldsymbol{v}_h\right\|_{\boldsymbol{L}^2(K_1^{\mathrm{f}})}^2 + \frac{1}{8}k^{-2}h\,[\![\gamma_{\mathrm{d}^*}(\alpha\mathrm{d}\boldsymbol{v}_h)]\!]^2\\ &\quad + \frac{1}{8}\left(4+16C_1^2k^{-2}\right)k^2h^{-1}\,\|[\![\gamma_{\mathrm{d}}\boldsymbol{v}_h]\!]\|_{\boldsymbol{L}^2(\mathrm{f})}^2.\end{aligned}$$

Summing the contributions from $\mathrm{f}\in\mathcal{S}_h$ and using $\lambda\ge 2+8C_1^2k^{-2}$ again, we have

$$\sum_{\mathrm{f}\in\mathcal{S}_h}\left|\int_{\mathrm{f}}\{\!\{\gamma_{\mathrm{d}^*}(\alpha\mathrm{d}\boldsymbol{v}_h)\}\!\}\cdot[\![\gamma_{\mathrm{d}}\boldsymbol{v}_h]\!]\right| \;\le\; \frac{1}{4}\|\boldsymbol{v}_h\|_{1,h}^2.\tag{20}$$

The first inequality in (16) is proven by inserting (19) and (20) into (17).

The second inequality in (16) can be proven by similar arguments and the Cauchy-Schwarz inequality. □

Theorem 3.3. *Suppose the penalty parameter $\lambda \ge 2+8C_1^2k^{-2}$. The discrete problem* (11) *has a unique solution.*

Proof. Since (11) is a linear and finite-dimensional problem, the existence and uniqueness of the solution come directly from Lemma 3.2. □

Remark 3.4. *For the NIPFEM, the last term in* (17) *vanishes. The coercivity of $\mathscr{A}_{\mathrm{d}}^h$ holds for any $\lambda>0$. While in the SIPFEM, the coercivity of $\mathscr{A}_{\mathrm{d}}^h$ relies on "sufficiently large" λ.*

4. A priori error estimates

This section is devoted to error estimates for finite element solutions. First we introduce the space of piecewise regular functions

$$\boldsymbol{H}^r(\Omega_1,\Omega_2)=\left\{\boldsymbol{v}\in\boldsymbol{L}^2(\Omega):\boldsymbol{v}|_{\Omega_j}\in\boldsymbol{H}^r(\Omega_j),\ j=1,2\right\},$$
$$\|\boldsymbol{v}\|_{\boldsymbol{H}^r(\Omega_1,\Omega_2)}:=\left(\|\boldsymbol{v}\|^2_{\boldsymbol{H}^r(\Omega_1)}+\|\boldsymbol{v}\|^2_{\boldsymbol{H}^r(\Omega_2)}\right)^{1/2},\qquad\forall\, r\geq 1.$$

4.1. Approximation property

In this subsection, we prove that the extended finite element space $\boldsymbol{U}^h(k;\mathrm{d})$ has optimal approximation property to $\boldsymbol{H}^{r+1}(\Omega_1,\Omega_2)$. First we cite [1] for the Sobolev extension and [9] for the approximation property of $\boldsymbol{U}^h(k;\mathrm{d})$ to $\boldsymbol{H}^{r+1}(\Omega)$.

Lemma 4.1 (Sobolev extension)**.** *Let $r\geq 1$. There exist two extension operators $\mathcal{E}_i:\boldsymbol{H}^{r+1}(\Omega_i)\to\boldsymbol{H}^{r+1}(\Omega)$, $i=1,2$, such that for each $\boldsymbol{u}_i\in\boldsymbol{H}^{r+1}(\Omega)$, $\mathcal{E}_i\boldsymbol{u}_i=\boldsymbol{u}_i$ in Ω_i and $\|\mathcal{E}_i\boldsymbol{u}_i\|_{\boldsymbol{H}^{r+1}(\Omega)}\leq C\,\|\boldsymbol{u}_i\|_{\boldsymbol{H}^{r+1}(\Omega_i)}$ with the constant $C=C(r,\Omega_i)$.*

Lemma 4.2. *Suppose $1\leq r\leq k$ and $0\leq m\leq r$. There exist an interpolation operator Π_{d}: $\boldsymbol{H}^{r+1}(\Omega)\to\boldsymbol{U}^h(k;\mathrm{d})$ and a constant $C>0$ independent of h such that, for any $\boldsymbol{u}\in\boldsymbol{H}^{r+1}(\Omega)$ and any $K\in\mathcal{T}_h$,*

$$\|\boldsymbol{u}-\Pi_{\mathrm{d}}\boldsymbol{u}\|_{\boldsymbol{H}^m(K)}+h\|\mathrm{d}(\boldsymbol{u}-\Pi_{\mathrm{d}}\boldsymbol{u})\|_{\boldsymbol{H}^m(K)}\leq Ch^{r+1-m}\|\boldsymbol{u}\|_{\boldsymbol{H}^{r+1}(K)}.$$

Now we define the interpolation operator $\Pi_{\mathrm{d,X}}$ onto the extended finite element space $\boldsymbol{U}^h(k;\mathrm{d})$. For any $\boldsymbol{u}\in\boldsymbol{H}^{r+1}(\Omega_1,\Omega_2)$, let $\boldsymbol{u}_i=\mathcal{E}_i\left(\boldsymbol{u}|_{\Omega_i}\right)\in\boldsymbol{H}^{r+1}(\Omega)$ be the extension of $\boldsymbol{u}|_{\Omega_i}$ to Ω. The interpolation $\Pi_{\mathrm{d,X}}\boldsymbol{u}\in\boldsymbol{U}^h(k;\mathrm{d})$ is defined by

$$\Pi_{\mathrm{d,X}}\boldsymbol{u}=\Pi_{\mathrm{d}}\boldsymbol{u}_i\quad\text{in }\Omega_i,\qquad i=1,2.\tag{21}$$

Lemma 4.3. *Suppose $r\geq 1$. There is a constant C independent of h such that*

$$|||\boldsymbol{u}-\Pi_{\mathrm{d,X}}\boldsymbol{u}|||_{1,h}\leq Ch^{\min(k,r)}\|\boldsymbol{u}\|_{\boldsymbol{H}^{r+1}(\Omega_1,\Omega_2)}\qquad\forall\,\boldsymbol{u}\in\boldsymbol{H}^{r+1}(\Omega_1,\Omega_2).$$

Proof. Let $\boldsymbol{u}_i=\mathcal{E}_i\left(\boldsymbol{u}|_{\Omega_i}\right)$ be the extension of $\boldsymbol{u}|_{\Omega_i}$ to Ω. Set $\boldsymbol{\zeta}=\boldsymbol{u}-\Pi_{\mathrm{d,X}}\boldsymbol{u}$ and $\boldsymbol{\zeta}_i=\boldsymbol{u}_i-\Pi^h_{\mathrm{d}}\boldsymbol{u}_i$, $i=1,2$. From Lemma 4.1, Lemma 4.2, and (21), we find that

$$\|\boldsymbol{\zeta}_i\|_{\boldsymbol{L}^2(\Omega)}+h\,\|\mathrm{d}\boldsymbol{\zeta}_i\|_{\boldsymbol{L}^2(\Omega)}\leq Ch^{\mu+1}\|\boldsymbol{u}\|_{\boldsymbol{H}^{r+1}(\Omega_i)},\qquad i=1,2,$$

where $\mu=\min(k,r)$. Since $\boldsymbol{\zeta}=\boldsymbol{\zeta}_i$ in Ω_i, this shows

$$\sum_{j=1}^{2}\left\|\alpha^{1/2}\mathrm{d}\boldsymbol{\zeta}\right\|^2_{\boldsymbol{L}^2(\Omega_j)}+\left\|\beta^{1/2}\boldsymbol{\zeta}\right\|^2_{\boldsymbol{L}^2(\Omega)}\leq Ch^{2\mu}\|\boldsymbol{u}\|^2_{\boldsymbol{H}^{r+1}(\Omega_1,\Omega_2)}.\tag{22}$$

The trace inequality in (15) shows

$$\begin{aligned}\mathscr{J}_0(\boldsymbol{\zeta},\boldsymbol{\zeta})&\leq Ch^{-1}\sum_{\mathrm{f}\in\mathcal{S}_h}\sum_{i=1}^{2}\left(h^{-1}\,\|\boldsymbol{\zeta}_i\|^2_{\boldsymbol{L}^2(K^{\mathrm{f}})}+\|\boldsymbol{\zeta}_i\|_{\boldsymbol{L}^2(K^{\mathrm{f}})}\,\|\nabla\boldsymbol{\zeta}_i\|_{\boldsymbol{L}^2(K^{\mathrm{f}})}\right)\\&\leq Ch^{2\mu}\sum_{\mathrm{f}\in\mathcal{S}_h}\sum_{i=1}^{2}\|\boldsymbol{u}_i\|^2_{\boldsymbol{H}^{r+1}(K^{\mathrm{f}})}\leq Ch^{2\mu}\|\boldsymbol{u}\|^2_{\boldsymbol{H}^{r+1}(\Omega_1,\Omega_2)}.\end{aligned}\tag{23}$$

Using similar arguments and replacing $\gamma_{\mathrm{d}}\boldsymbol{\zeta}$ with $\gamma_{\mathrm{d}^*_\succ}(\beta\boldsymbol{\zeta})$, we also have

$$\mathscr{J}_2(\boldsymbol{\zeta},\boldsymbol{\zeta}) = \sum_{\mathrm{f}\in\mathcal{S}_h} \frac{k^2}{h} \left\| \left[\!\left[\gamma_{\mathrm{d}^*_\succ}(\beta\boldsymbol{\zeta})\right]\!\right] \right\|^2_{\boldsymbol{L}^2(\mathrm{f})} \le Ch^{2\mu}\|\boldsymbol{u}\|^2_{\boldsymbol{H}^{r+1}(\Omega_1,\Omega_2)}. \tag{24}$$

To estimate the rest terms in $|||\boldsymbol{\zeta}|||_{1,h}$, we recall from (10) that α is constant in $K\cap\Omega_j$ for any $K\in\mathcal{T}_{h,\Sigma}$. Then Lemma 4.2 and (15) yield

$$\begin{aligned}\|\gamma_{\mathrm{d}^*}(\alpha\mathrm{d}\boldsymbol{\zeta}|_{\Omega_i})\|^2_{\boldsymbol{L}^2(\mathrm{f})} &\le C\left(h^{-1}\|\alpha\mathrm{d}\boldsymbol{\zeta}_i\|^2_{\boldsymbol{L}^2(K^{\mathrm{f}})} + \|\alpha\mathrm{d}\boldsymbol{\zeta}_i\|_{\boldsymbol{L}^2(K^{\mathrm{f}})}\|\nabla(\alpha\mathrm{d}\boldsymbol{\zeta}_i)\|_{\boldsymbol{L}^2(K^{\mathrm{f}})}\right)\\ &\le Ch^{2\mu-1}\|\boldsymbol{u}_i\|^2_{\boldsymbol{H}^{r+1}(K^{\mathrm{f}})}.\end{aligned}$$

Counting all $\mathrm{f}\in\mathcal{S}_h$ and using the definition of $\mathscr{J}_1$, we infer that

$$\mathscr{J}_1(\boldsymbol{\zeta},\boldsymbol{\zeta}) + \sum_{\mathrm{f}\in\mathcal{S}_h}\frac{h}{\lambda k^2}\|\{\!\{\gamma_{\mathrm{d}^*}(\alpha\mathrm{d}\boldsymbol{\zeta})\}\!\}\|^2_{\boldsymbol{L}^2(\mathrm{f})} \le Ch^{2\mu}\|\boldsymbol{u}\|^2_{\boldsymbol{H}^{r+1}(\Omega_1,\Omega_2)}. \tag{25}$$

The proof is completed by inserting (22)–(25) into the definition of $|||\boldsymbol{\zeta}|||^2_{1,h}$. □

4.2. Error estimates in discrete energy norm

First we provide a modified Céa's lemma for the approximation error. The proof follows the same lines as in the well-known Céa's lemma.

Lemma 4.4. *Let $\boldsymbol{u}$, $\boldsymbol{u}_h$ be the solutions to* (1) *and* (11) *respectively. Then*

$$|||\boldsymbol{u}-\boldsymbol{u}_h|||_{1,h} \le 9\inf_{\boldsymbol{v}_h\in\boldsymbol{U}^h(k;\mathrm{d})}|||\boldsymbol{u}-\boldsymbol{v}_h|||_{1,h}.$$

Proof. For any $\boldsymbol{v}_h\in\boldsymbol{U}^h(k;\mathrm{d})$, write $\boldsymbol{\eta}_h=\boldsymbol{u}_h-\boldsymbol{v}_h$. Using Lemma 3.2 and the Galerkin orthogonality (13), we find that

$$|||\boldsymbol{\eta}_h|||^2_{1,h} \le 4\mathscr{A}^h_{\mathrm{d}}(\boldsymbol{\eta}_h,\boldsymbol{\eta}_h) = 4\mathscr{A}^h_{\mathrm{d}}(\boldsymbol{u}-\boldsymbol{v}_h,\boldsymbol{\eta}_h) \le 8\,|||\boldsymbol{u}-\boldsymbol{v}_h|||_{1,h}\,|||\boldsymbol{\eta}_h|||_{1,h},$$

This shows $|||\boldsymbol{\eta}_h|||_{1,h} \le 8\,|||\boldsymbol{u}-\boldsymbol{v}_h|||_{1,h}$. Then the proof is finished by using the triangle equality and the arbitrariness of $\boldsymbol{v}_h$. □

Choosing $\boldsymbol{v}_h=\Pi_{\mathrm{d,X}}\boldsymbol{u}$ in Lemma 4.4 and using Lemma 4.3, we immediately get the error estimate for both SIPFEM and NIPFEM.

Theorem 4.5. *There is a constant C independent of h such that*

$$|||\boldsymbol{u}-\boldsymbol{u}_h|||_{1,h} \le Ch^{\min(k,r)}\|\boldsymbol{u}\|_{\boldsymbol{H}^{r+1}(\Omega_1,\Omega_2)}, \qquad r\ge 1.$$

4.3. $\boldsymbol{L}^2$-error estimate for SIPFEM

We will use the duality technique to estimate the error $\boldsymbol{e}=\boldsymbol{u}-\boldsymbol{u}_h$ in $\boldsymbol{L}^2$-norm. Consider the auxiliary problem:

$$\text{Find } \boldsymbol{w}\in\boldsymbol{H}_0(\mathrm{d},\Omega): \quad (\alpha\mathrm{d}\boldsymbol{w},\mathrm{d}\boldsymbol{v})+(\beta\boldsymbol{w},\boldsymbol{v}) = (\beta\boldsymbol{e},\boldsymbol{v}) \quad \forall\,\boldsymbol{v}\in\boldsymbol{H}_0(\mathrm{d},\Omega). \tag{26}$$

The Lax-Milgram lemma shows that (26) has a unique solution. Moreover, the arbitrariness of $\boldsymbol{v}$ implies that

$$\left[\!\left[\gamma_{\mathrm{d}^*}(\alpha\mathrm{d}\boldsymbol{w})\right]\!\right]=0, \quad \left[\!\left[\gamma_{\mathrm{d}^*_\succ}(\beta\boldsymbol{w}-\beta\boldsymbol{e})\right]\!\right]=0 \quad \text{on } \Sigma. \tag{27}$$

Theorem 4.6. *Assume the solution of* (26) *is piecewise regular and satisfies*

$$\|\boldsymbol{w}\|_{\boldsymbol{H}^2(\Omega_1,\Omega_2)} \leq C \|\boldsymbol{e}\|_{\boldsymbol{L}^2(\Omega)}. \tag{28}$$

There exists a constant C independent of h such that

$$\|\boldsymbol{u}-\boldsymbol{u}_h\|_{\boldsymbol{L}^2(\Omega)} \leq Ch^{\min(k,r)+1}\|\boldsymbol{u}\|_{\boldsymbol{H}^{r+1}(\Omega_1,\Omega_2)}.$$

Proof. Since $\boldsymbol{w} \in \boldsymbol{H}^2(\Omega_1,\Omega_2) \cap \boldsymbol{H}_0(\mathrm{d},\Omega)$, taking $\boldsymbol{v}=\boldsymbol{e}$ in (26) and using (27) and the Galerkin orthogonality (13), we find that

$$(\beta\boldsymbol{e},\boldsymbol{e}) + \mathscr{J}_2(\boldsymbol{e},\boldsymbol{e}) = \mathscr{A}_{\mathrm{d}}^h(\boldsymbol{w},\boldsymbol{e}) = \mathscr{A}_{\mathrm{d}}^h(\boldsymbol{e},\boldsymbol{w}-\Pi_{\mathrm{d,X}}\boldsymbol{w}). \tag{29}$$

Using Lemma 4.3 and Theorem 4.5, we obtain

$$(\beta\boldsymbol{e},\boldsymbol{e}) \quad \leq \quad 2\,|||\boldsymbol{e}|||_{1,h}\,|||\boldsymbol{w}-\Pi_{\mathrm{d,X}}\boldsymbol{w}|||_{1,h} \leq Ch^{1+\min(k,r)}\|\boldsymbol{w}\|_{\boldsymbol{H}^2(\Omega_1,\Omega_2)}\|\boldsymbol{u}\|_{\boldsymbol{H}^{r+1}(\Omega_1,\Omega_2)}.$$

The proof is finished by using (28). □

4.4. $\boldsymbol{L}^2$-error estimate for NIPFEM

Let $\boldsymbol{e}=\boldsymbol{u}-\boldsymbol{u}_h$ be the error function for the NIPFEM and $\boldsymbol{w} \in \boldsymbol{H}_0(\mathrm{d})$ be the solution of (26) associated with $\boldsymbol{e}$.

Theorem 4.7. *Suppose assumption* (28) *holds. There exists a constant C independent of h such that*

$$\|\boldsymbol{u}-\boldsymbol{u}_h\|_{\boldsymbol{L}^2(\Omega)} \leq Ch^{\min(k,r)+1/2}\|\boldsymbol{u}\|_{\boldsymbol{H}^{r+1}(\Omega_1,\Omega_2)}.$$

Proof. The proof follows closely that of Theorem 4.6. We only present the sketch here. As done in (29),

$$\begin{aligned}(\beta\boldsymbol{e},\boldsymbol{e}) + \mathscr{J}_2(\boldsymbol{e},\boldsymbol{e}) = \mathscr{A}_{\mathrm{d}}^h(\boldsymbol{w},\boldsymbol{e}) &= \mathscr{A}_{\mathrm{d}}^h(\boldsymbol{e},\boldsymbol{w}) + 2\sum_{\mathrm{f}\in\mathcal{S}_h}\int_{\mathrm{f}} \{\!\{\gamma_{\mathrm{d}^*}(\alpha\mathrm{d}\boldsymbol{w})\}\!\}\,[\![\gamma_{\mathrm{d}}\boldsymbol{e}]\!] \\ &= \mathscr{A}_{\mathrm{d}}^h(\boldsymbol{e},\boldsymbol{e}_{\boldsymbol{w}}) + 2\sum_{\mathrm{f}\in\mathcal{S}_h}\int_{\mathrm{f}} \{\!\{\gamma_{\mathrm{d}^*}(\alpha\mathrm{d}\boldsymbol{w})\}\!\}\,[\![\gamma_{\mathrm{d}}\boldsymbol{e}]\!],\end{aligned} \tag{30}$$

where $\boldsymbol{e}_{\boldsymbol{w}}=\boldsymbol{w}-\Pi_{\mathrm{d,X}}\boldsymbol{w}$. Similar to the proof of Theorem 4.6, the first term on the right-hand side satisfies

$$\mathscr{A}_{\mathrm{d}}^h(\boldsymbol{e},\boldsymbol{e}_{\boldsymbol{w}}) \leq Ch^{\min(k,r)+1}\|\boldsymbol{u}\|_{\boldsymbol{H}^{r+1}(\Omega_1,\Omega_2)}\|\boldsymbol{w}\|_{\boldsymbol{H}^2(\Omega_1,\Omega_2)}. \tag{31}$$

Using the trace inequality (15), the second term can be estimated as follows:

$$\begin{aligned}\left|\sum_{\mathrm{f}\in\mathcal{S}_h}\int_{\mathrm{f}} \{\!\{\gamma_{\mathrm{d}^*}(\alpha\mathrm{d}\boldsymbol{w})\}\!\}\,[\![\gamma_{\mathrm{d}}\boldsymbol{e}]\!]\right| &\leq \sum_{\mathrm{f}\in\mathcal{S}_h}\|\{\!\{\gamma_{\mathrm{d}^*}(\alpha\mathrm{d}\boldsymbol{w})\}\!\}\|_{\boldsymbol{L}^2(\mathrm{f})}\,[\![\gamma_{\mathrm{d}}\boldsymbol{e}]\!] \\ &\leq C\frac{h^{1/2}}{k\lambda^{1/2}}\mathscr{J}_0(\boldsymbol{e},\boldsymbol{e})^{1/2}\,\|\{\!\{\gamma_{\mathrm{d}^*}(\alpha\mathrm{d}\boldsymbol{w})\}\!\}\|_{\boldsymbol{L}^2(\Sigma)} \\ &\leq Ch^{\min(k,r)+1/2}\|\boldsymbol{u}\|_{\boldsymbol{H}^{r+1}(\Omega_1,\Omega_2)}\|\boldsymbol{w}\|_{\boldsymbol{H}^2(\Omega_1,\Omega_2)}.\end{aligned} \tag{32}$$

The proof is finished by inserting (31) and (32) into (30) and using (28). □

It is worth remarking that the $\boldsymbol{L}^2$-error estimate for the SIPFEM is optimal with respect to h, while it is suboptimal for the NIPFEM with half an order deteriorated. However, the optimal convergence rate of NIPFEM are observed in $\boldsymbol{L}^2(\Omega)$-norm for all numerical experiments.

5. Numerical experiments

The purpose of this section is to verify the optimal h-convergence rates of the proposed finite element methods for $\boldsymbol{H}(\mathrm{d};\Omega)$-elliptic interface problems. Our implementation is based on the adaptive finite element package " Parallel Hierarchical Grid " (PHG) [40] and the computations are carried out on the cluster LSSC-IV of the State Key Laboratory on Scientific and Engineering Computing, Chinese Academy of Sciences.

Note that $\mathcal{T}_h$ is a quasi-uniform tetrahedral mesh of Ω. The intersection of the curved interface with $\mathcal{T}_h$ can yield very general shapes of sub-domains. Numerical quadratures on curved domains and curved interfaces play a very important role in designing high-order finite element methods. In [3], we have developed highly accurate numerical quadratures to deal with these issues. The numerical quadratures are used in the implementation of the numerical experiments here. The order of numerical quadratures is set to $p = 2k + 3$ for $\boldsymbol{U}^h(k, \mathrm{d})$.

We only present the numerical results for NIPFEM. The results of SIPFEM are similar. The computational domain is set to $\Omega = (0, 1)^3$ which is subdivided successively into tetrahedral finite element meshes $\mathcal{T}_h$ (Fig. 3). The interface Σ for Example 5.1–5.3 is the sphere of radius 0.25 and centered at $(0.5, 0.5, 0, 5)$ (see Fig. 2), where the one for Fig. 5.4 consists of two touching spheres of radius 0.1 and centered at $(0.4, 0.5, 0.5)$, $(0.6, 0.5, 0.5)$ respectively (Fig. 4). The coefficients of partial differential equations are set by

$$\alpha = \beta = 1 \quad \text{in } \Omega_1, \qquad \alpha = \beta = 100 \quad \text{in } \Omega_2.$$

The penalty parameter is set by $\lambda = 1$.

The convergence rates are tested for

$$\Theta_0 := \left\| \sqrt{\beta}(\boldsymbol{u} - \boldsymbol{u}_h) \right\|_{\boldsymbol{L}^2(\Omega)} \left\| \sqrt{\beta}\boldsymbol{u} \right\|^{-1}_{\boldsymbol{L}^2(\Omega)}, \quad \Theta_1 := |||\boldsymbol{u} - \boldsymbol{u}_h|||_{\boldsymbol{H}(\mathrm{d},\Omega)} \, |||\boldsymbol{u}|||^{-1}_{\boldsymbol{H}(\mathrm{d},\Omega)},$$

where $|||\boldsymbol{v}|||^2_{\boldsymbol{H}(\mathrm{d},\Omega)} := \sum_{i=1}^2 \|\sqrt{\alpha}\mathrm{d}\boldsymbol{v}\|^2_{\boldsymbol{L}^2(\Omega_i)} + \left\|\sqrt{\beta}(\boldsymbol{u} - \boldsymbol{u}_h)\right\|^2_{\boldsymbol{L}^2(\Omega)}$. On each mesh, the number of tetrahedra is denoted by N_{ele} and the number of degrees of freedom is denoted by N_{dof}.

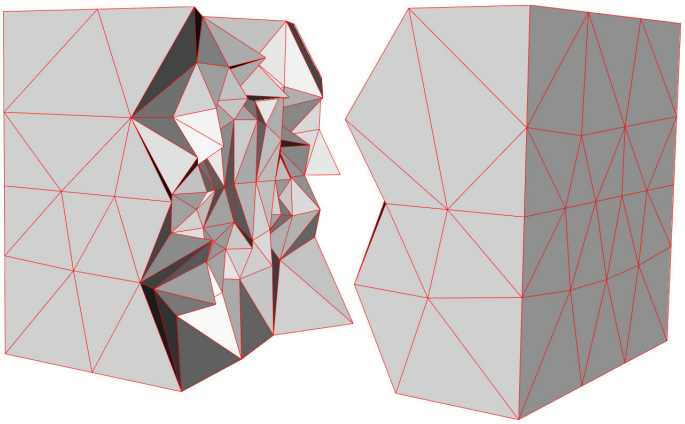

Figure 3: A tetrahedral mesh of the computational domain Ω.

Example 5.1. *The purpose of this example is to verify the convergence rate of the finite element method for H^1–interface problem, that is,* $\mathrm{d} = \mathbf{grad}$. *The analytical solution is given by*

$$u(x,y,z) = \begin{cases} e^{xyz} & in\ \Omega_1, \\ \sin(x+y+z) & in\ \Omega_2. \end{cases}$$

Table 1 shows that, both relative errors decay optimally with respect to mesh size for polynomial degrees $k = 1, 2, 3$, namely,

$$\Theta_0 \sim h^{k+1} \sim N_{\mathrm{ele}}^{-(k+1)/3}, \qquad \Theta_1 \sim h^k \sim N_{\mathrm{ele}}^{-k/3}.$$

This confirms the theoretical results in Theorem 4.5 and Theorem 4.7. For the relative $|||\cdot|||_{\boldsymbol{L}^2(\Omega)}$–error, we observe a super convergence of order $\mathcal{O}\left(h^{1/2}\right)$ compared to the theoretical result. We note that this super convergence is also observed in [39].

Table 1: Convergence rates for H^1-interface problem (Example 5.1)

$k=1$					
N_{ele}	N_{dof}	Θ_1	Order	Θ_0	Order
768	189	2.142e-01	—	2.258e-02	—
6,144	1,241	1.058e-01	1.02	8.247e-03	1.45
49,152	9,009	4.151e-02	1.35	1.140e-03	2.85
393,216	68,705	1.800e-02	1.21	2.766e-04	2.04
$k=2$					
N_{ele}	N_{dof}	Θ_1	Order	Θ_0	Order
768	1,241	3.568e-03	–	1.436e-04	–
6,144	9,009	8.187e-04	2.12	1.427e-05	3.33
49,152	68,705	1.959e-04	2.06	1.606e-06	3.15
393,216	536,769	4.830e-05	2.02	1.785e-07	3.17
$k=3$					
N_{ele}	N_{dof}	Θ_1	Order	Θ_0	Order
768	3,925	2.696e-04	—	5.485e-06	—
6,144	58,898	3.433e-05	2.97	3.019e-07	4.18
49,152	228,241	4.328e-06	2.99	1.798e-08	4.07
393,216	179,7409	5.427e-07	3.00	1.078e-09	4.06

Example 5.2. *The purpose of this example is to verify the convergence rate of the finite element method for $H(\mathbf{curl})$–interface problem. The exact solution is given by*

$$\boldsymbol{u} = \begin{cases} \boldsymbol{u}_1 & in\ \Omega_1, \\ \boldsymbol{u}_2 & in\ \Omega_2, \end{cases}$$

where

$$\boldsymbol{u}_1(x,y,z) = \Big(-\cos x^2 e^{-y^2}\sin(2\pi z), -\cos y^2 e^{-x^2}\sin(2\pi z), \cos y^2 e^{-z^2}\sin(2\pi x)\Big)^\top,$$
$$\boldsymbol{u}_2(x,y,z) = \Big(-\sin x^2 e^{y^2}\cos(2\pi z), -\sin y^2 e^{x^2}\cos(2\pi z), \sin y^2 e^{z^2}\cos(2\pi x)\Big)^\top.$$

Table 2 shows that Θ_0 and Θ_1 satisfy the asymptotic behaviors

$$\Theta_0 \sim h^{k+1} \sim N_{\text{ele}}^{-(k+1)/3}, \quad \Theta_1 \sim h^k \sim N_{\text{ele}}^{-k/3}, \quad k = 1,2,3.$$

The results confirm the theoretical results in Theorem 4.5 and Theorem 4.7 for $\boldsymbol{H}(\mathbf{curl}, \Omega_1, \Omega_2)$–interface problems.

Table 2: Convergence rates for $\boldsymbol{H}(\mathbf{curl})$-interface problem (Example 5.2)

$k=1$					
N_{ele}	N_{dof}	Θ_1	Order	Θ_0	Order
768	2,104	3.155e-01	—	1.604e+00	—
6,144	15,536	1.205e-01	1.39	4.197e-01	1.93
49,152	119,392	4.845e-02	1.31	1.062e-01	1.98
393,216	936,128	2.196e-02	1.14	2.696e-02	1.98
$k=2$					
N_{ele}	N_{dof}	Θ_1	Order	Θ_0	Order
768	8,052	5.205e-02	—	2.100e-01	—
6,144	61,320	9.146e-03	2.50	2.510e-02	3.06
49,152	478,608	1.981e-03	2.20	3.236e-03	2.96
393,216	3,781,920	4.687e-04	2.07	4.124e-04	2.97
$k=3$					
N_{ele}	N_{dof}	Θ_1	Order	Θ_0	Order
768	20,336	4.519e-03	—	1.316e-02	—
6,144	157,024	5.597e-04	3.01	9.648e-04	3.77
49,152	1,234,112	6.543e-05	3.10	6.187e-05	3.96

Example 5.3. *The purpose of this example is to verify the convergence rate of the finite element method for $H(\text{div})$–interface problem. The exact solution $\boldsymbol{u}$ is same to the solution in Example 5.2.*

Again Table 3 shows that Θ_0 and Θ_1 satisfy the asymptotic behaviors

$$\Theta_0 \sim h^{k+1} \sim N_{\text{ele}}^{-(k+1)/3}, \quad \Theta_1 \sim h^k \sim N_{\text{ele}}^{-k/3}, \quad k = 1,2,3.$$

The results confirm the theoretical results in Theorem 4.5 and Theorem 4.7 for $\boldsymbol{H}(\text{div}, \Omega_1, \Omega_2)$–interface problems.

Table 3: Convergence rates for $\boldsymbol{H}(\mathrm{div})$-interface problem (Example 5.3)

$k=1$					
N_{ele}	N_{dof}	Θ_1	Order	Θ_0	Order
768	4,896	2.857e-01	—	7.669e-01	—
6,144	3,8016	7.371e-02	1.95	1.929e-01	1.99
49,152	299,520	1.910e-02	1.94	4.934e-02	1.97
393,216	2,377,728	5.609e-03	1.77	1.240e-02	1.99
$k=2$					
N_{ele}	N_{dof}	Θ_1	Order	Θ_0	Order
768	14,400	4.453e-02	—	6.240e-02	—
6,144	112,896	7.789e-03	2.52	7.896e-03	2.98
49,152	893,952	1.415e-03	2.46	9.846e-04	3.00
393,216	7,114,752	3.079e-04	2.20	1.234e-04	2.99
$k=3$					
N_{ele}	N_{dof}	Θ_1	Order	Θ_0	Order
768	31,680	3.969e-03	—	5.275e-03	—
6,144	249,600	4.225e-04	3.23	3.243e-04	4.02
49,152	1,981,440	4.956e-05	3.09	2.065e-05	3.97

Example 5.4 (Two tangential spheres)**.** *This example investigates the NIPFEM for the $\boldsymbol{H}(\mathbf{curl},\Omega)$–interface problem with complicated interface. Here the interface Σ is the union of two touching spheres which have radius* 0.1 *and are centered at* $(0.4,0.5,0.5)^\top$ *and* $(0.6,0.5,0.5)^\top$ *respectively (see Fig. 4). The exact solution is same to the solution in Example 5.2.*

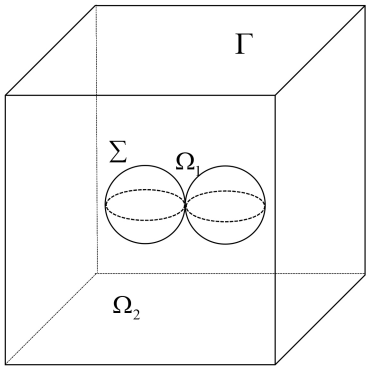

Figure 4: The interface consists of two touching spheres.

In this example, Ω_1 is a non-convex domain and is the union of two open balls tangential to each other at $(0.5,0.5,0.5)$. Table 4 displays the relative errors and the convergence rates. Once more we get optimal convergence rates of discrete solutions in both $\boldsymbol{L}^2(\Omega)$-norm and energy norm.

Table 4: Convergence rates of of NIPFEM for $\boldsymbol{H}(\mathbf{curl}, \Omega)$ problem II (*Example* 5.4)

$k=1$					
N_{ele}	N_{dof}	Θ_1	Order	Θ_0	Order
768	2,104	4.426e-01	—	2.894e+00	—
6,144	15,536	1.424e-01	1.64	7.686e-01	1.91
49,152	119,392	5.063e-02	1.49	1.884e-01	2.03
393,216	936,128	2.205e-02	1.20	4.694e-02	2.00
$k=2$					
N_{ele}	N_{dof}	Θ_1	Order	Θ_0	Order
768	8,052	5.679e-02	—	2.804e-01	—
6,144	61,320	9.111e-03	2.64	3.202e-02	3.13
49,152	478,608	1.975e-03	2.21	3.985e-03	3.01
393,216	3,781,920	4.681e-04	2.08	4.910e-04	3.02
$k=3$					
N_{ele}	N_{dof}	Θ_1	Order	Θ_0	Order
768	20,336	5.924e-03	—	3.205e-02	—
6,144	157,024	5.406e-04	3.45	1.082e-03	4.89
49,152	1,234,112	6.462e-05	3.06	6.661e-05	4.02

6. Conclusion

In this paper, we propose a unified framework for analyzing high-order interface penalty finite element methods for H^1-, $\boldsymbol{H}(\mathbf{curl})$-, and $\boldsymbol{H}(\text{div})$-elliptic interface problems on unfitted meshes. We supplement the continuous with appropriate interface conditions which guarantees the well-posedness of continuous problems and inspires us to add adequate interface penalties to the bilinear forms of discrete variational problems. Optimal convergence rates of the finite element methods are proven in both energy norm and $\boldsymbol{L}^2$-norm by means of duality techniques. All finite element error estimates are independent of the location of the interface relative to the meshes. Extensive numerical experiments with smooth solutions are presented to verify the optimal convergence of discrete solutions.

References

[1] R. Adams, Sobolev Spaces, Academic Press, 1975.

[2] A. Buffa, M. Costabel, D. Sheen, On traces for $\boldsymbol{H}(\mathbf{curl}, \Omega)$ in Lipschitz domains, Journal of Mathematical Analysis and Applications, 276 (2002) 845–867.

[3] T. Cui, W. Leng, H. Liu, L. Zhang, W. Zheng, High-order numerical quadratures in a tetrahedron with an implicitly defined curved interface, ACM Transactions on Mathematical Software, 46 (2019), 1–18.

[4] A. Hansbo, P. Hansbo, An unfitted finite element method, based on Nitsche's method for elliptic interface problems, Computer Methods in Applied Mechanics and Engineering, 191 (2002) 5537–5552.

[5] R. Massjung, An unfitted discontinuous Galerkin method applied to elliptic interface problems, SIAM Journal on Numerical Analysis, 50 (2012) 3134–3162.

[6] Z. Chen, Y. Xiao, L. Zhang, The adaptive immersed interface finite element method for elliptic and Maxwell interface problems, Journal of Computational Physics, 228 (2009) 5000–5019.

[7] H. Wu, Y. Xiao, An unfitted hp-interface penalty finite element method for elliptic interface problems, arXiv preprint, arXiv:1007.2893.

[8] P. Huang, H. Wu, Y. Xiao, An unfitted interface penalty finite element method for elliptic interface problems, Computer Methods in Applied Mechanics and Engineering, 323 (2017) 439–460.

[9] P. Monk, Finite Element Methods for Maxwell's Equations, Oxford University Press, 2003.

[10] Z. Chen, Q. Du, J. Zou, Finite element methods with matching and nonmatching meshes for Maxwell's equations with discontinuous coefficients, SIAM Journal on Numerical Analysis, 37 (2000) 1542–1570.

[11] R. Hiptmair, J. Li, J. Zou, Convergence analysis of finite element methods for $\boldsymbol{H}(\mathbf{curl}, \Omega)$-elliptic interface problems, Numerische Mathematik, 122 (2012) 557–578.

[12] R. Hiptmair, J. Li, J. Zou, Convergence analysis of finite element methods for $\boldsymbol{H}(\mathrm{div}, \Omega)$-elliptic interface problems, Journal of Numerical Mathematics, 18 (2010) 187–218.

[13] E. Burman, P. Zunino, Numerical approximation of large contrast problems with the unfitted Nitsche method, Frontiers in Numerical Analysis – Durham 2010, Lecture Notes in Computational Science and Engineering 85, J. Blowey and M. Jensen (eds.), 227–282, 2012.

[14] C.S. Peskin, The immersed boundary method, Acta Numerica, 11 (2002) 479–517.

[15] Z. Li, The immersed interface method using a finite element formulation, Applied Numerical Mathematics, 27 (1998) 253–267.

[16] R.J. LeVeque, Z. Li, The immersed interface method for elliptic equations with discontinuous coefficients and singular sources, SIAM Journal on Numerical Analysis, 31 (1994) 1019–1044.

[17] R.P. Fedkiw, T. Aslam, B. Merriman, S. Osher, A non-oscillatory Eulerian approach to interfaces in multimaterial flows (the ghost fluid method), Journal of Computational Physics, 152 (1999) 457–492.

[18] C. Chu, I.G. Graham, T. Hou, A new multiscale finite element method for high-contrast elliptic interface problems, Mathematics of Computation, 79 (2010) 1915–1955.

[19] I. Babuška, The finite element method for elliptic equations with discontinuous coefficients, Computing, 5 (1970) 207–218.

[20] Y. Zhou, S. Zhao, M. Feig, G. Wei, High order matched interface and boundary (MIB) schemes for elliptic equations with discontinuous coefficients and singular sources, Journal of Computational Physics, 231 (2006) 1–30.

[21] N. Moës, J. Dolbow, T. Belytschko, A finite element method for crack growth without remeshing, International Journal for Numerical Methods in Engineering, 46 (1999) 131–150.

[22] R. Becker, E. Burman, P. Hansbo, A Nitsche extended finite element method for incompressible elasticity with discontinuous modulus of elasticity, Computer Methods in Applied Mechanics and Engineering, 198 (2009) 3352–3360.

[23] C. Lehrenfeld, A. Reusken, Optimal preconditioners for Nitsche-XFEM discretizations of interface problems, Numerische Mathematik, 135 (2017) 313–332.

[24] E. Burman, S. Claus, P. Hansbo, M. G. Larson, A. Massing, CutFEM: discretizing geometry and partial dierential equations, International Journal for Numerical Methods in Engineering,104 (2015) 472–501.

[25] S.P.A. Bordas, E. Burman, M.G. Larson, M.A. Olshanskii, Geometrically Unfitted Finite Element Methods and Applications, Lecture Notes in Computational Science and Engineering 121, Springer, 2017.

[26] A. Hansbo, P. Hansbo, A finite element method for the simulation of strong and weak discontinuities in solid mechanics, Computer Methods in Applied Mechanics and Engineering, 193 (2004) 3523–3540.

[27] J.D. Sanders, J.E. Dolbow, T.A. Laursen, On the methods for stabilizing constraints over enriched interfaces in elasticity, International Journal for Numerical Methods in Engineering, 78 (2009) 1009–1036.

[28] A. Massing, M.G. Larson, A. Logg, M.E. Rognes, A stabilized Nitsche overlapping mesh method for the Stokes problem, Numerische Mathematik, 128 (2014) 73–101.

[29] E. Burman, S. Claus, A. Massing, A stabilized cut finite element method for the three field Stokes problem, SIAM Journal on Scientific Computing, 37 (2015) 1705–1726.

[30] L. Cattaneo, L. Formaggia, G. F. Iori, A. Scotti, P. Zunino, Stabilized extended finite elements for the approximation of saddle point problems with unfitted interfaces, Calcolo, 52 (2014) 1–30.

[31] A. Massing, B. Schott, W. Wall, A stabilized Nitsche cut finite element method for the Oseen problem, Computer Methods in Applied Mechanics and Engineering, 328 (2018) 262–300.

[32] M. Winter, B. Schott, A. Massing, W. Wall, A Nitsche cut finite element method for the Oseen problem with general Navier boundary conditions, Computer Methods in Applied Mechanics and Engineering, 330 (2017) 220–252.

[33] M. Kirchhart, S. Gro, A. Reusken, Analysis of an XFEM discretization for Stokes interface problems, SIAM Journal on Scientific Computing, 38 (2016) 1019–1043.

[34] J. Guzmán, M. Olshanskii, Inf-sup stability of geometrically unfitted Stokes finite elements, Mathematics of Computation, 87 (2017) 2091–2112.

[35] S. Gross, A. Reusken, Numerical Methods for Two-phase Incompressible Flows, Springer Series in Computational Mathematics 40, Springer, 2011.

[36] A. Massing, M.G. Larson, A. Logg, M. Rognes, A Nitsche-based cut finite element method for a fluid-structure interaction problem, Communications in Applied Mathematics and Computational Science, 10 (2015) 97–120.

[37] C. Annavarapu, M. Hautefeuille, J.E. Dolbow, A robust Nitsche's formulation for interface problems, Computer Methods in Applied Mechanics and Engineering, 225 (2012) 44–54.

[38] N. Barrau, R. Becker, E. Dubach, R. Luce, A robust variant of NXFEM for the interface problem, Comptes Rendus Mathematique, 350 (2012) 789–792.

[39] E. Burman, A penalty free non-symmetric Nitsche type method for the weak imposition of boundary conditions, SIAM Journal on Numerical Analysis, 50 (2012) 1959–1981.

[40] L. Zhang, A parallel algorithm for adaptive local renement of tetrahedral meshes using bisection, Numerical Mathematics Theory Methods and Applications, 2 (2009) 65–89. (http://lsec.cc.ac.cn/phg)